# Hubbard Model on the Infinite Dimensional Diamond Lattice

*Thesis submitted for the degree of*
*Magister Philosophiae*

*Condensed Matter Sector*

CANDIDATE:
Marco G. Airoldi

SUPERVISORS:
Dott. Giuseppe Santoro
Dott. Sandro Sorella

NOVEMBER 1992

# 1 Introduction

The study of interacting fermionic lattice models in the limit of large spatial dimension has been devoted a rapidly growing attention in the past few years. [1] The interest in these techniques arises primarily because the resulting theory is much simpler than the corresponding one in any finite dimension, whereas the physics retained by the model is still non trivial.

The Hubbard hamiltonian has certainly been the most studied model in the infinite dimensional limit. As for the types of lattices which have been studied, recent investigations have focused on the hyper-cubic lattice at $D = \infty$ and on the Bethe lattice with infinite coordination number. [2, 3, 4]

We report here an application of these techniques to the $\infty$-dimensional generalization of the honeycomb ($D = 2$) or diamond ($D = 3$) lattices. To fix the notation, we write the Hubbard hamiltonian as follows

$$H = -\tilde{t} \sum_{\mathbf{R}\in A,\{\mathbf{e}^i\}} \sum_{\sigma} \left[ c^{+}_{\mathbf{R}+\mathbf{e}^i,\sigma}\, c_{\mathbf{R},\sigma} + H.c. \right] + U \sum_{\mathbf{R}\in A \bigoplus B} n_{\mathbf{R},\uparrow}\, n_{\mathbf{R},\downarrow} \,, \qquad (1)$$

where the bipartite nature of the lattices under consideration allows us to identify two sublattices $A$ and $B$, and $\{\mathbf{e}^i\}$ is a set of vectors connecting a site in $A$ to its nearest-neighbors in $B$. In generalizing the honeycomb/diamond lattices in higher dimensions we will require that each site has $D + 1$ nearest-neighbors and that the angle between any two of the $D + 1$ vectors $\{\mathbf{e}^i\}$ is a constant (which turns out to be $-1/D$). The set of vectors $\{\mathbf{e}^i\}$ is constructed in Appendix A, but their explicit form is quite immaterial in many respects. It is crucial, however, that the resulting lattice has no inversion symmetry (i.e., $-\mathbf{e}^i$ does not connect to any neighbor), at variance with the hyper-cubic case.

The common feature of this class of lattices, in any dimension $D \geq 2$, is a vanishing density of states (DOS) at the Fermi energy for the half-filled case, $\rho(E) \propto |E|$, which results in a semi-metallic behaviour (at least in a single-particle picture). At $D = \infty$ the density of states becomes particularly simple, and reads:

$$\rho(E) = \frac{|E|}{t} e^{-E^2/2t^2} \,, \qquad (2)$$

where $t$ is an energy scale in terms of which the original hopping parameter has been scaled as $\tilde{t} = (2/D)^{1/2} t$, a procedure which ensures that the kinetic energy does not dominate on the interaction as $D \to \infty$. (See Appendix B for a derivation of Eq. 2, and Fig. 1 for a comparison between $\rho$ in $D = 2, 3$ and in $D = \infty$.)

As in any half-filled bipartite lattice, for $U \to \infty$ - where the model maps into an unfrustrated Heisenberg model with Antiferromagnetic (AF) nearest-neighbor coupling $J = 4\tilde{t}^2/U$ - the ultimate fate of the Ground State (GS) is to show a Neel type of AF long-range order. In the hyper-cubic case in any $D \geq 2$, the Mean-Field (MF)

critical value of $U$ for the transition to a Neel antiferromagnet is actually vanishing ($U_c = 0$), because of the prefect nesting properties of the half-filled Fermi surface. In contrast, in the present case, as a result of the vanishing DOS at the Fermi level, the MF value of $U_c$ for the AF transition is pushed to a finite value $U_c > 0$. [5] That this MF description is at least qualitatively correct even in $D = 2$ seems to be confirmed by the Quantum Monte Carlo (QMC) simulation for the honeycomb lattice of Ref. [5]. Quantum fluctuations increase the actual value of $U_c$. In $D = 2$, $U_c(T = 0)$ is found to be roughly a factor 2 bigger than the MF value - $U_c/\tilde{t} \approx 4 \div 5$, whereas $U_c^{(MF)}/\tilde{t} = 2.23$. [5]

A finite value of $U_c$ makes the situation interesting and potentially rich of surprises. First, there is a finite window of values of $U$ around $U = 0$ in which the paramagnetic GS should be stable, and one can ask the question of possible violations of Fermi Liquid Theory, especially in $D = 2$. The answer to such a question is very difficult, although no hint has been seen to date for such a scenario in $D = 2$. In $D = \infty$, the situation is in this respect more clear (but also less surprising), and Fermi Liquid Theory should apply without problems. Secondly, one can envisage the possibility of a (Semi)Metal-Insulator transition separate from the magnetic transition and occurring at some other value of $U$, in contrast to the MF picture. In $D = 2$ this seems *not to be the case*. [5] One of the motivations for the present study was the hope of clarifying, or confirming, some of these points.

The essence of our approach to the $D = \infty$ limit of this class of models is very similar to the ones already appeared in the literature, and is briefly discussed, for completeness, in the next section. It suffices here to say that a mapping into a self-consistent Anderson impurity problem [6] allows us to calculate the local Green's function $G_{ii\sigma}$ in a quite reliable way, by either a one-impurity Quantum Monte Carlo simulation or a surprisingly good perturbative approach.

Single particle properties are straightforwardly obtained from the Green's function. As for the response functions, we have used two alternative approaches: (1) We can calculate charge and spin susceptibilities by using the irreducible two-particle vertex parts, obtained from the one-impurity QMC simulation, in the full Bethe-Salpeter equation for the lattice problem, as done in Ref. [2]. This approach is quite intensive numerically and we have used it only as a check. (2) If one is interested only in q = 0 properties, for instance in the compressibility $\partial n/\partial \mu$ and the staggered susceptibility $\chi_{sp} = \partial M/\partial H_S$, one has just to take the appropriate derivatives of $n$ and $M$ - which can be directly calculated from $G$ - including, in the case of $\chi_{sp}$, a staggered Zeeman field in the hamiltonian. This is, up to now, the only strategy available to calculate such quantities within the perturbative approach, for lack of a reliable way of calculating two-particle Green's functions. It is, on the other hand, not very sensible within the Monte Carlo approach since the data are plagued by statistical errors, which make the calculation of *derivatives* quite cumbersome.

The (preliminary) $(U, T)$ phase diagram for the model at half-filling is shown in Fig. 2. The most prominent feature is the expected magnetic transition to a Neel

AF. At $T = 0$ we estimate $U_c/t \approx 2.1$, whereas a MF theory predicts (at $D = \infty$) a value $U_c^{(MF)}/t = 1.596$. Evidently, quantum fluctuations are not quite as effective as in $D = 2$ in pushing the $U_c(T = 0)$ towards a higher value. The disagreement between the MF (Stoner) theory prediction for the Neel temperature $T_N(U)$ (shown in Fig. 2 by the dotted curve) and the actual result (tentatively sketched by the solid curve) is more and more pronounced as $U$ increases. In particular, the former has a large $U$ behaviour which is totally wrong, $T_N^{(MF)}(U) \propto U$, whereas the correct result is expected to be proportional to the strength of the exchange coupling of a spin to the shell of nearest-neighbors, $DJ_D = 4D\tilde{t}^2/U \propto t^2/U$. (The conventional MF theory on the Heisenberg model becomes, on the contrary, exact in infinite dimension.)

As for the nature of the magnetic transition, the critical exponents $\beta$ and $\gamma$ for the order parameter $M(T)$ and the susceptibility $\chi_{sp}(T)$ are virtually indistinguishable - not too surprisingly - from the Ginzburg-Landau MF predictions $\beta = 1/2$, $\gamma = 1$.

One interesting point to discuss is the possibility of a genuine semi-metal/insulator Mott transition *not driven by the onset of the magnetic long range order*, i.e. if the two transitions might occur at different values of $U_c$. By studying the compressibility $\partial n/\partial \mu$ at half filling as a function of temperature, we clearly see the opening of a gap below $T_N$ for all the $U$ studied. It seems, therefore, that the antiferromagnet is also an insulator, as perhaps expected from a MF picture.

In the next two sections we will first give more details on the method used to tackle the problem, and then present some of the results obtained so far. Four appendices, devoted to the illustration of technical points, end this report.

# 2 The method

A crucial simplification of the Hubbard model at $D = \infty$ consists in the fact that the self-energy function $\Sigma$ becomes site-diagonal, a property which can be proved using the methods of Ref. [7] with minor modifications due to the presence of phase-factors in the off-diagonal Green's functions. A derivation of the arguments upon which this remarkable property is based is given in Appendix C.

Given this fundamental locality of $\Sigma$, the gist of the method consists in mapping the lattice problem into a self-consistent Anderson impurity problem. The relevant equations describing this mapping are formally identical to the ones reported in the literature for the hypercubic and the Bethe lattice, [2, 3, 4] and we report them here for completeness. The local Green's function is obtained by the solution of a local problem

$$G_{ii\sigma}(i\omega_n) = [{\mathcal{G}^o_{ii\sigma}}^{-1}(i\omega_n) - \Sigma_{i\sigma}(i\omega_n)]^{-1} , \qquad (3)$$

where $\Sigma_{i\sigma}[\mathcal{G}^o]$ is the local self-energy corresponding to the given $\mathcal{G}^o$, $\mathcal{G}^o$ being an auxiliary local Green's function which plays the role, formally, of a non-interacting Green's function for the local problem, but actually embodies correlation effects due to the

surrounding lattice. The crucial requirement that fixes the choice of $\mathcal{G}^o$ is that the resulting $\Sigma_{i\sigma}[\mathcal{G}^o]$ and $G_{ii\sigma}$ *coincide with the actual self-energy and local Green's function for the lattice problem.* This requirement imposes the self-consistency condition

$$G_{ii\sigma}(i\omega_n) = \int_0^\infty dE\ \rho(E)\ \frac{Z_\sigma^{\bar{\alpha}}}{Z_\sigma^A Z_\sigma^B - E^2}\ , \tag{4}$$

where

$$Z_\sigma^\alpha = i\omega_n + \mu + (-1)^R \sigma H_S - \Sigma_\sigma^{(\alpha)}(i\omega_n)\ . \tag{5}$$

($\bar{\alpha}$ denotes sublattice $B$ if $\alpha = A$ and viceversa.) Eqs. (4) is nothing but a disguised form of the Dyson equation which relates $G$ and $\Sigma$ for the lattice problem. A derivation of Eqs. (3-5) is illustrated in Appendix D. (Notice that in the above equations we have allowed for the presence of a staggered magnetic field $H_S$ which is useful to calculate the staggered susceptibilty of the model.) The only difference with the hypercubic case is the non-interacting density of states $\rho(E)$ appearing in Eq. (4) which is given in the present case by Eq. (2).

The strategy to solve the problem is then the following. One starts from an arbitrary auxiliary function $\mathcal{G}^o$ and *solves the local problem* to get, say, $\Sigma$. (The QMC would actually furnish $G$.) The result obtained is not, however, the actual self-energy for the lattice problem as the two alternative expressions for $G$ in Eqs. (3) and (4) do not in general coincide. We then calculate $G$ from Eq. (4) and invert Eq. (3) to solve for an improved $\mathcal{G}^o$. We iterate this procedure until self-consistency is reached, i.e. Eqs. (3) and (4) are both satisfied.

The hard part of the problem is clearly the local problem, i.e., how to get $\Sigma$ from a local (arbitrary) $\mathcal{G}^o$. Several techniques have been developped during the years to solve this Anderson impurity problem. In principle, an exact answer is obtained by performing a single-impurity Quantum Monte Carlo simulation using, for instance, the Hirsh and Fye algorithm at finite temperature. [8] Alternatively, any reliable perturbative scheme can be used. Among the possible schemes, a very simple perturbative approach appear to give answers in good agreement with the Monte Carlo results - sometimes even for $U/t$ as large as 8 - at least within the paramagnetic phase. It consists in approximating $\Sigma_{i\sigma}[\mathcal{G}^o]$ with the simple second-order diagram where $\mathcal{G}^o$ is used as a propagator. [9] More explicitly, we take:

$$\Sigma_{\alpha\sigma}(i\omega_n) = U\ \langle n_{\alpha\bar{\sigma}} \rangle + U^2\ \frac{1}{\beta} \sum_{\omega_B} \mathcal{G}^o_{\alpha\sigma}(i\omega_n - i\omega_B)\chi_o^{(\bar{\sigma}\bar{\sigma})}(i\omega_B)\ , \tag{6}$$

with

$$\chi_o^{(\sigma\bar{\sigma})}(i\omega_B) = \frac{1}{\beta} \sum_{\omega_m} \mathcal{G}^o_{\alpha\bar{\sigma}}(i\omega_m)\mathcal{G}^o_{\alpha\bar{\sigma}}(i\omega_m + i\omega_B)\ , \tag{7}$$

where the first term, $U\ \langle n_{\alpha\sigma} \rangle$, corresponds to the Hartree diagram and would lead, in absence of any further correction, to the Mean Field approximation. It is crucial to stress that $\mathcal{G}^o$ - and not $G$ or the non-interacting Green's function $G^o$ - is used in these expressions. The agreement with the QMC is quite poor, in fact, if $G$

or $G^o$ are used, except for very small $U$ ($U/t \approx 1$). The algorithm is most easily implemented at finite temperature by working directly on the imaginary axis and using fast Fourier transforms to perform the convolutions involving the Matsubara frequencies. (Alternatively, for the paramagnetic case we have adopted a real axis $T = 0$ approach which furnishes direct information on the spectral density. [10])

# 3 Some results

Fig. 3 shows a comparison between the Monte Carlo data (solid squares) and the perturbative results obtained using Eq. (6) (solid line) for the *paramagnetic* imaginary time Green's function $G(\tau)$ at $\beta = 8$. Notice how the agreement is surprisingly good even for $U/t$ as large as 8 (a slightly larger discrepancy is obtained for $U/t = 6$, shown in the inset).

To date, most of our results have been obtained using this simpler perturbative approach, although there are definite indications that the Neel temperature curve, for instance, is not quantitatively correct for $U \geq 4$ (see dashed curve in Fig. 2). We have in fact calculated the staggered susceptibility by using the QMC two-particle local Green's function into the full Bethe-Salpeter for the lattice problem. The results, although qualitatively similar to the ones obtained by the perturbative approach, indicate that the Neel temperature is underestimated for $U \geq 4$ by the latter method. The QMC prediction for the Neel temperature is indicated by the open squares in Fig. 2, the solid line being a guide to the eye.

The procedure adopted to calculate the compressibility $\partial n/\partial \mu$ and the staggered susceptibility $\chi_{sp} = \partial M/\partial H_S$, within the perturbative approach is quite straightforward. $n$ and $M$ can in fact be directly calculated, for any given chemical potential $\mu$ or staggered field $H_S$, from the imaginary time local Green's function

$$n = 2 + \sum_{\sigma} G_{A\sigma}(\tau = 0^+) , \tag{8}$$

$$M = G_{A\downarrow}(\tau = 0^+) - G_{A\uparrow}(\tau = 0^+) . \tag{9}$$

Fig. 4 shows the staggered susceptibility $\chi_{sp}(T)$ as a function of $T$ for $U/t = 4$. A divergence occurs at $T_N \approx 0.18$, below which a non-vanishing spontaneous magnetization sets in, as shown in Fig. 5. The transition shows MF critical exponents for both $\chi_{sp}$ and $M(T)$, i.e., $\gamma = 1$ and $\beta = 1/2$. The behaviour of the compressibilty in the same range of temperature is shown in Fig. 6. Clearly, the compressibility drops very quickly below the Neel temperature as one would expect if a charge gap has been opened. Indeed, in a single particle picture, a gap $\Delta$ results in a compressibility of the form

$$\left.\frac{\partial n}{\partial \mu}\right|_{\text{half filling}} \approx \text{const}\; T^{\nu}\, e^{-\Delta/T} , \tag{10}$$

which well fits our results as shown in the inset of Fig. 6. In the Semi-metallic phase, on the contrary, the compressibility is expected to go linearly to zero as $T \to 0$, $\partial n/\partial \mu \propto T$, a behaviour which is indeed found for $U/t = 2$ and is illustrated by the solid circles in Fig. 6.

The issue of a "genuine" Mott transition, not driven by AF long range order, has been quite debated in the recent literature and certainly deserves a few concluding remarks. If we decide to ignore the possibility of the onset of AF long range order by *not looking at the right response function* (i.e. the staggered susceptibility, which happens to diverge at some point), we would keep finding paramagnetic solutions of our self-consistent equations (3)-(4) for the Green's function which would appear to be perfectly legitimate, i.e. the one-particle Green's function is totally blind, in this respect, to the occurrence of any critical phenomenon. By insisting on a paramagnetic solution, the system would sooner or later open a gap, upon increase of $U$, by breaking the Fermi liquid: this is nothing but the Mott transition dealt with in Refs. [3, 4]. For the model we are considering, this happens (at $T = 0$) at $U_c/t \approx 8.5$. As $U$ approaches this critical value the effective mass of the quasiparticles would diverge, and a gap would be opened in the spectrum. It is worth stressing, however, that for the nearest-neighbor hopping bipartite lattices considered so far, such a paramagnetic solution is actually *unstable* in the region where the Mott transition would occur, as one can verify by applying a small magnetic field. The actual relevance of a genuine Mott transition would be therefore confined, so far, to models in which the disorder inhibits AF long range order. [11]

# Appendices

## A Defining the hyper-diamond lattice

The hyper-diamond lattice in D dimensions can be defined as a bipartite lattice satisfying the following two conditions:

- Each point in the lattice has $D+1$ nearest neighbors at a distance $a$ (which we take hereafter to set the unit of length, $a = 1$), belonging to the opposite sublattice.
- Denoting by $\{\mathbf{e}^i\}_D$ the set of $D+1$ unit vectors connecting a point of the lattice to its nearest neighbors, the angle between any two vectors $\mathbf{e}^i$ and $\mathbf{e}^j$ is a constant:

$$\mathbf{e}^i \cdot \mathbf{e}^j = \alpha_D \qquad \forall i \neq j \; . \tag{11}$$

This definition reduces, for instance, to the honeycomb lattice for $D = 2$ ($\alpha_2 = -\frac{1}{2} = \cos 120^o$). For $D = 3$ it coincides with the diamond lattice ($\alpha_3 = -\frac{1}{3} \approx \cos 109^o$). We will show that the constant $\alpha_D$ is given, in any dimension, by $\alpha_D = -\frac{1}{D}$.

*Proof.* (By induction.) Suppose that $\{\tilde{\mathbf{e}}^i\}_{D-1}$ is a set of $D$ unit vectors in $D-1$ dimensions satisfying the condition (11). We will now construct the required set of vectors $\{\mathbf{e}^i\}_D$ in $D$ dimensions as follows:

$$\begin{aligned} \mathbf{e}^i &= (\gamma\, \tilde{\mathbf{e}}^i, \alpha_D) \qquad\qquad i = 1, 2, ..., D \\ \mathbf{e}^{D+1} &= \underbrace{(0, 0, 0, 0, \cdots, 0, 1)}_{D+1} \end{aligned} \tag{12}$$

where the first $D-1$ components of each vector $\mathbf{e}^i$ ($i = 1, 2, ..., D$) coincide with the corresponding components of $\tilde{\mathbf{e}}^i$ scaled by a common factor $\gamma$, the last component being equal to $\alpha_D$. Simple algebra shows that the condition (11) is verified and the vectors $\mathbf{e}^i$ are normalized to one, provided we require:

$$\begin{aligned} \gamma &= \sqrt{1 - \alpha_D^2} \\ \alpha_D &= \frac{\alpha_{D-1}}{1 - \alpha_{D-1}} \; . \end{aligned} \tag{13}$$

It is now easy to verify, by direct substitution, that $\alpha_D = -\frac{1}{D}$ is the only solution of Eq. (13) with initial condition $\alpha_{D=2} = \cos 120^o$, which completes the proof.

This proof provides also an iterative method to construct the set of vectors $\{\mathbf{e}^i\}_D$ in $D$ dimensions. One can even start from $D = 1$ where the hyper-diamond degenerates into:

$$\{\mathbf{e}^i\}_{D=1} = \{\mathbf{e}^1 = (1,0)\,,\ \mathbf{e}^2 = (0,1)\}\,, \tag{14}$$

and construct lattices of higher dimension using Eqs. (12) and (13). Note, in passing, that the vectors $\{\mathbf{e}^i\}_D$ become orthogonal as $D \to \infty$.

# B Hubbard model on the hyper-diamond lattice: Definitions and Mean-Field approximation

The Hubbard Hamiltonian on a bipartite lattice can be written as:

$$H = -\tilde{t} \sum_{\mathbf{R}\in A,\mathbf{e}^i} \sum_{\sigma} [c^+_{\mathbf{R},\sigma}\, c_{\mathbf{R}+\mathbf{e}^i,\sigma} + H.c.] + U \sum_{\mathbf{R}\in A \bigoplus B} n_{\mathbf{R},\uparrow}\, n_{\mathbf{R},\downarrow} \tag{15}$$

where R stands for a generic site of sublattice A, and $\mathbf{e}^i$ indicates any of the $D+1$ vectors connecting a site in A to its nearest-neighbors in B. ($n_{\mathbf{R},\sigma} = c^+_{\mathbf{R},\sigma}\, c_{\mathbf{R},\sigma}$ is the number operator.) In D dimensions, the unitary cell is defined by the vectors:

$$\mathbf{a}_i = \mathbf{e}^{D+1} - \mathbf{e}^i \qquad\qquad i = 1,2,...,D \tag{16}$$

and the reciprocal basis vectors are defined by the relation $\mathbf{a}_i \cdot \mathbf{b}_j = 2\pi\delta_{ij}$.

The hamiltonian for $U = 0$ can be diagonalized in two steps. We first revert from Wannier states to Bloch waves:

$$c^+_{A\mathbf{k},\sigma} = \frac{1}{\sqrt{N}} \sum_{\mathbf{R}\in A} e^{-i\,\mathbf{k}\cdot\mathbf{R}} c^+_{\mathbf{R},\sigma} \tag{17}$$

$$c^+_{B\mathbf{k},\sigma} = \frac{1}{\sqrt{N}} \sum_{\mathbf{R}\in A} e^{-i\,\mathbf{k}\cdot(\mathbf{R}+\mathbf{d})} \cdot c^+_{\mathbf{R}+\mathbf{d},\sigma}\,, \tag{18}$$

where N is the number of lattice cells, and $\mathbf{d} = \mathbf{e}^{D+1}$. Using this transformation the hamiltonian becomes partially diagonal (A and B operators are still coupled) and reads:

$$H_{U=0} = -t \sum_{\mathbf{k}}^{BZ} [A_{\mathbf{k}}\, c^+_{A\mathbf{k},\sigma}\, c_{B\mathbf{k},\sigma} + A^*_{\mathbf{k}}\, c^+_{B\mathbf{k},\sigma}\, c_{A\mathbf{k},\sigma}]\,, \tag{19}$$

where the sum over k runs over the first Brillouin zone, and

$$A_{\mathbf{k}} = \sum_{j=1}^{D+1} e^{-i\,\mathbf{k}\cdot\mathbf{e}^j}\,. \tag{20}$$

The diagonalization of $H_{U=0}$ is then carried out by defining a new set of creation and destruction operators: ($n = 1,2$)

$$\psi_{n\mathbf{k},\sigma} \;=\; u_{n\mathbf{k}}\, c_{A\mathbf{k},\sigma} + v_{n\mathbf{k}}\, c_{B\mathbf{k},\sigma}\,, \tag{21}$$

where the coefficients are subject to the canonicity restriction $|u_{n\mathbf{k}}|^2 + |v_{n\mathbf{k}}|^2 = 1$, and selected in such a way as to put $H_{U=0}$ in the form:

$$H_{U=0} = \sum_{\mathbf{k}}^{BZ} \sum_{n,\sigma} E_{n\mathbf{k}}\, \psi^{+}_{n\mathbf{k},\sigma}\, \psi_{n\mathbf{k},\sigma} \,. \tag{22}$$

The band energies $E_{n\mathbf{k}}$ turn out to be given by

$$E_{n\mathbf{k}} = \pm \tilde{t} \mid A_{\mathbf{k}} \mid , \tag{23}$$

which, expressing the momentum as $\mathbf{k} = \sum_j k_j \mathbf{b}_j$, can be rewritten in the form

$$|E_{n\mathbf{k}}| = \tilde{t}\, |A_{\mathbf{k}}| = \tilde{t}\, |1 + \sum_{j=1}^{D} e^{i\, 2\pi k_j}| = \sqrt{X^2 + Y^2} \qquad k_j \in (0,1) \,, \tag{24}$$

$X$ and $Y$ being defined by

$$\begin{aligned} X &= \tilde{t} \left( 1 + \sum_{j=1}^{D} \cos 2\pi k_j \right) \\ Y &= \tilde{t} \sum_{j=1}^{D} \sin 2\pi k_j \,. \end{aligned} \tag{25}$$

The crucial step is now to apply the central limit theorem to Eq. (25). The probability distributions for the variables $X$ and $Y$ become gaussians in the limit of large dimension and are given by

$$P_X(X) = \frac{1}{\sqrt{\pi\, \tilde{t}^2\, D}}\, e^{-\frac{(X-\bar{t})^2}{\tilde{t}^2\, D}} \tag{26}$$

$$P_Y(Y) = \frac{1}{\sqrt{\pi\, \tilde{t}^2\, D}}\, e^{-\frac{Y^2}{\tilde{t}^2\, D}} \,. \tag{27}$$

It is then clear that, in order to obtain a model having a non trivial limit for $D \to \infty$, the parameter $\tilde{t}$ in the kinetic energy must be scaled so as to make the variance of the distributions $P_X$ and $P_Y$ equal to a finite non-vanishing constant $t$ at $D = \infty$, i.e.

$$\tilde{t} = \sqrt{\frac{2}{D}}\, t \,. \tag{28}$$

Rewriting $\tilde{t}$ in terms of $t$ and sending $D \to \infty$, we get that the limiting distributions for $X$ and $Y$ actually coincide ($P_X = P_Y = P$),

$$P(X) = \frac{1}{\sqrt{2\pi\, t^2}}\, e^{-\frac{X^2}{2\, t^2}} \,, \tag{29}$$

and the distribution for the energy (i.e. the density of states) becomes:

$$\rho(E) = \int dX\, dY\; P(X)\; P(Y)\; \delta(E - \sqrt{X^2 + Y^2}) = \frac{|E|}{t^2}\, e^{-\frac{E^2}{2\, t^2}} \tag{30}$$

Notice that the density of states goes to zero for $E \to 0$.

We will now give a brief account of the mean-field treatment of the full Hubbard Hamiltonian. The Hartree-Fock mean field theory can be obtained by approximating the exact interaction operator in Eq. (15), as a bilinear form

$$H_{int} = U \sum_{\mathbf{R} \in A \bigoplus B} \langle n_{\mathbf{R},\uparrow} \rangle \, n_{\mathbf{R},\downarrow} + n_{\mathbf{R},\uparrow} \, \langle n_{\mathbf{R},\downarrow} \rangle \, , \tag{31}$$

where the averages $\langle n_{\mathbf{R},\sigma} \rangle$ have to be determined self-consistently. To study a Neel-type of antiferromagnetic long-range order at half filling, the choice $\langle n_{\mathbf{R},\sigma} \rangle = \frac{1}{2} + (-1)^R \, \sigma \, \frac{M}{2}$ is made, where the notation $(-1)^R$ stands for $+1$ on sublattice A and $-1$ on B. It is easy to demonstrate that, within this approximation, the system has a gap $\Delta$ which is related to $U$ by the equation:

$$U \int_0^\infty dE \, \rho(E) \, \frac{1}{\sqrt{E^2 + \Delta^2}} \, \tanh(\frac{\beta}{2} \sqrt{E^2 + \Delta^2}) = 1 \, , \tag{32}$$

where $\beta = \frac{1}{T}$, and $T$ is the temperature. The critical value $U_c$ of the interaction $U$ which determines the transition between the paramagnetic-metallic phase ($\Delta = 0$) and antiferromagnetic-insulating phase is therefore defined by:

$$U_c \int_0^\infty dE \, \rho(E) \frac{1}{|E|} \, \tanh(\frac{\beta}{2} \, |E|) \, = 1 \tag{33}$$

which is easily calculated at $T = 0$, giving:

$$\frac{U_c}{t}(T = 0) = \frac{4}{\sqrt{2 \, \pi}} \approx 1.596 \tag{34}$$

When $U$ is less than $U_c$, the system is paramagnetic and semimetallic ($\Delta = 0$) while for $U$ larger than $U_c$ the system becomes antiferromagnetic and insulating.

# C Momentum independence of the Self Energy

In this section we want to show that the self-energy, $\Sigma(\mathbf{k}, \omega_n)$, becomes independent of the momentum $\mathbf{k}$, in the limit of infinite dimension. In order to prove this statement we will first consider the behaviour of the non-interacting Green's function $G^o_{\alpha\beta}(i,j)$ for $D \to \infty$. The Green's function $G^o_{\alpha\beta}(i,j)$ can be expressed in terms of its Fourier transform by the relation:

$$G^o_{\alpha\beta}(\mathbf{R} = \mathbf{R}_i - \mathbf{R}_j \in A, \omega) \, = \, \int_{BZ} \frac{d^D\mathbf{k}}{(2\pi)^D} e^{i \, \mathbf{k} \cdot \mathbf{R}} \, G^o_{\alpha\beta}(\mathbf{k}, \omega) \tag{35}$$

where $G^o_{\alpha\beta}$ are given by the relations:

$$G^o_{AA}(\mathbf{k}, \omega) \;\; = \;\; G^o_{BB}(\mathbf{k}, \omega) \; = \; \frac{1}{2} \, [G^o_1(\mathbf{k}, \omega) + G^o_2(\mathbf{k}, \omega)] \tag{36}$$

$$G^o_{AB}(\mathbf{k},\omega) = e^{i\,\phi_{\mathbf{k}}}\,\frac{1}{2}\,[G^o_1(\mathbf{k},\omega) - G^o_2(\mathbf{k},\omega)] \tag{37}$$

$$G^o_{BA}(\mathbf{k},\omega) = e^{-i\,\phi_{\mathbf{k}}}\,\frac{1}{2}\,[G^o_1(\mathbf{k},\omega) - G^o_2(\mathbf{k},\omega)] \tag{38}$$

with:

$$G^o_i(\mathbf{k},\omega) = \frac{1}{i\,\omega + \mu - E_i(\mathbf{k})} \qquad e^{i\,\phi_{\mathbf{k}}} = \frac{A_{\mathbf{k}}}{|A_{\mathbf{k}}|} \tag{39}$$

and $E_1(\mathbf{k}) = -t\ |A_{\mathbf{k}}|$, $E_2(\mathbf{k}) = t\ |A_{\mathbf{k}}|$. We will first consider the component $G^o_{AA}(\mathbf{R},\omega)$ of the Green's function. Due to the fact that $G^o_{AA}(\mathbf{k},\omega)$ depends on $\mathbf{k}$ only through $E(\mathbf{k})$, it is possible to incorporate the momentum integration in the function:

$$v^{AA}_{\mathbf{R}}(E) = \int_{BZ} \frac{d^D\mathbf{k}}{(2\pi)^D}\,\delta(E - E_{\mathbf{k}})\,e^{i\,\mathbf{k}\cdot\mathbf{R}}\,, \tag{40}$$

in terms of which Eq. (35) reads:

$$G^o_{AA} = \int dE\ v^{AA}_{\mathbf{R}}(E)\ G^o_{AA}(E,\omega)\,. \tag{41}$$

The behaviour of $v^{AA}_{\mathbf{R}}$ can be analysed by taking the its Fourier transform with respect to $E$

$$\Psi_{\mathbf{R}}(s) = \int dE\ e^{i\,s\,E}\ v^{AA}_{\mathbf{R}}(E) = \int_{BZ} \frac{d^D\mathbf{k}}{(2\pi)^D}\ e^{i\,(s\,E(\mathbf{k}) + \mathbf{k}\cdot\mathbf{R})}\,. \tag{42}$$

Clearly, for $\mathbf{R} = 0$ $\Psi_{\mathbf{R}}(s)$ becomes the Fourier transform of the density of state $\rho(E)$, while for any other value of $\mathbf{R}$ belonging to sublattice A, it vanishes like $1/D$ or faster in the limit of infinite dimension. In fact, when $\mathbf{R}$ is a nearest-neighbor (in A) of the lattice point $\mathbf{R} = 0$, $\Psi_{\mathbf{R}}(s)$ can be rewritten as:

$$\begin{aligned}
\Psi_{\mathbf{R}=\mathbf{a}^j}(s) &= \int_{BZ} \frac{d^D\mathbf{k}}{(2\pi)^D}\ e^{i\,s\,E(\mathbf{k})}\ e^{i\,2\pi k_j} \\
&= \frac{1}{D}\int_{BZ} \frac{d^D\mathbf{k}}{(2\pi)^D}\ e^{i\,s\,E(\mathbf{k})}\ \sum_{j=1}^{D} e^{i\,2\pi k_j} \\
&= \frac{1}{D}\int_{BZ} \frac{d^D\mathbf{k}}{(2\pi)^D}\ e^{i\,s\,E(\mathbf{k})}\ \left[\frac{\sqrt{D}}{\sqrt{2}t}\,(X + iY) - 1\right]\,,
\end{aligned} \tag{43}$$

where the variables $X$ and $Y$ have been introduced in Appendix B, and $t$ is the scaled hopping parameter. Introducing, in the limit of $D \to \infty$, the gaussian distributions $P(X)$ and $P(Y)$ in the integral, we can rewrite:

$$\begin{aligned}
\Psi_{\mathbf{R}=\mathbf{a}^j}(s) &= \frac{1}{D}\int_{-\infty}^{+\infty} dX\,dY\,P(X)\,P(Y)\,e^{i\,s\,\sqrt{X^2+Y^2}}\ \left[\frac{\sqrt{D}}{\sqrt{2}t}\,(X + iY) - 1\right] \\
&\approx \text{const}\ O(\frac{1}{D})\,,
\end{aligned} \tag{44}$$

since the integral of the $(X + iY)$ term vanishes by parity.

The main consequence of this result is that the Green's function $G^o_{AA}(\mathbf{R},\omega)$ for $D \to \infty$ can be expressed as:

$$G^o_{AA}(\mathbf{R},\omega) = \delta_{\mathbf{R},0}\, G^o_{AA}(\omega) + O(\frac{1}{D})\,. \tag{45}$$

It is important to note that the $\mathbf{R} \neq 0$ terms in the Green's function $G^o_{AA}(\mathbf{R},\omega)$ can turn out to be non negligible anywhere there is a sum over $\mathbf{R}$ because, in this case, factors of $1/D$ can be compensated by the sum, giving a finite result. (For instance, the inverse-Fourier transform of Eq. (45), which is the non-interacting Green's function $G^o_{AA}(\mathbf{k},\omega)$ in the momentum space, depends of the momentum $\mathbf{k}$.)

The previous demonstration can be repeated, with some little modification, also for the off-diagonal component $G^o_{AB}$ of the Green's function. In this case, $G^o_{AB}$ depends of the momentum $\mathbf{k}$ through the energy $E(\mathbf{k})$ and the phase-factor $\phi_{\mathbf{k}}$. The corresponding function $v^{AB}_{\mathbf{R}}$ is then given by:

$$v^{AB}_{\mathbf{R}}(E) = \int_{BZ} \frac{d^D\mathbf{k}}{(2\pi)^D}\, \delta(E - E_{\mathbf{k}})\, e^{i\,(\mathbf{k}\cdot\mathbf{R} + \phi_{\mathbf{k}})} \tag{46}$$

and its Fourier transform reads:

$$\Psi_{\mathbf{R}}(s) = \int_{BZ} \frac{d^D\mathbf{k}}{(2\pi)^D}\, e^{i\,(s\,E(\mathbf{k}) + \mathbf{k}\cdot\mathbf{R} + \phi_{\mathbf{k}})}\,. \tag{47}$$

The value of $\Psi_{\mathbf{R}}(s)$ for a nearest-neighbor site, i.e., $\mathbf{R} = 0$ (recall that $\mathbf{R}$ in our convention belongs always to sublattice A), is given by:

$$\Psi_{\mathbf{R}=0}(s) = \int_{BZ} \frac{d^D\mathbf{k}}{(2\pi)^D}\, e^{i\,s\,E(\mathbf{k})}\, e^{i\phi_{\mathbf{k}}} \approx \mathrm{const} O(\frac{1}{\sqrt{D}})\,, \tag{48}$$

where steps similar to the ones used to arrive at Eq. (44) have been made. In a similar way one can show that every non site-diagonal term in $(G^o_{AB}, G^o_{AB})$ vanishes at least as $1/\sqrt{D}$ for $D \to \infty$.

Using the previous result, we can now analyse the locality property of the self-energy in $D = \infty$. We will consider only the second order diagram in $U$ but the argument can be easily generalized to all orders in $U$ with a little effort. The second order contribution to the self energy is represented by the diagram:

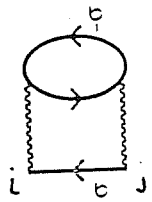


The analytic expression associated with this diagram is (the label $\alpha$ and $\beta$ denote sublattice A or B):

$$\Sigma_{\alpha\beta}(ij)(\omega) = G^o_{\alpha\beta}(i,j)\, G^o_{\alpha\beta}(i,j)\, G^o_{\beta\alpha}(j,i) = \tag{49}$$

$$= \delta_{ij}\, \Sigma_{\alpha\beta}(ii)(\omega) + O(\frac{1}{D^{3/2}}) \tag{50}$$

and the corresponding Fourier transform is given by:

$$\Sigma_{\alpha\beta}(\mathbf{k},\omega) = \sum_{\mathbf{R}\in A} e^{-i\,\mathbf{k}\cdot\mathbf{R}}\,\Sigma_{\alpha\beta}(ij)(\omega) = \Sigma_{\alpha\beta}(\omega) + O(\frac{1}{D^{1/2}})\,. \tag{51}$$

A similar argument can be applied to any n-th order *irreducible* self-energy diagram. In this case, $n-2$ internal lattice-site sums together with $2n-1$ internal $G^o$-lines conspire to make the formal leading correction to the momentum independence of order $1/\sqrt{D}$, as in Eq. (51). Thus the self-energy becomes local (i.e., momentum independent) for $D=\infty$, a property which introduces a considerable simplification in the theory.

Note, finally, that the independence of the momentum $\mathbf{k}$ is true only for an irreducible diagram. To appreciate why this is so, consider, for instance, the following reducible fourth-order diagram

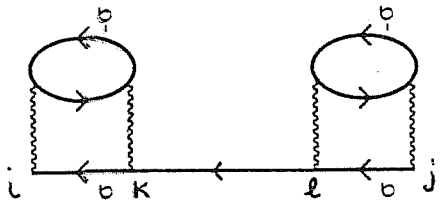


Formally, this diagram has $2n-2=2$ internal site sums and $2n-1=7$ internal lines, exactly as a fourth order irreducible diagram. In this case, however, we can write the double sum over the internal vertex $k$ and $l$ in terms of lower order irreducible self-energy diagrams as follows:

$$[\text{Reducible Diagram}] \;=\; \sum_{k,l} \Sigma^{(2)}_{ik}\, G^o(k,l)\, \Sigma^{(2)}_{lj}\,. \tag{52}$$

If we consider, in this sum, the term which corresponds to the labels $k=i$ and $l=j$ we obtain, for $i\neq j$, the contribution:

$$[\text{Term with } k=i, l=j] \;=\; \Sigma^{(2)}_{ii}\, G^o(i,j)\, \Sigma^{(2)}_{jj} \;\approx\; O(\frac{1}{\sqrt{D}})\,, \tag{53}$$

which is non-negligible when transformed back in momentum space.

# D Reduction to a local problem

In this section we will sketch the argument which allows to write the local Green's function as the self-consistent solution of a local problem. There are many possible approaches to get to the final result. Our proof is based on the ideas contained in Ref. [2].

The starting point is the Dyson equation for the Green's function. Due to the locality in space of the self-energy function ($\Sigma_{ij} = 0$ for $i \neq j$) we can clearly write

$$G_{ij\sigma} = G^o_{ij\sigma} + \sum_l G^o_{il\sigma}\Sigma_{l\sigma}G_{lj\sigma} \,. \tag{54}$$

Let us now define an auxiliary Green's function $\mathcal{G}^o_{ij\sigma}$ which satisfies a similar Dyson equation with a restriction in the lattice sum as follows:

$$\mathcal{G}^o_{ij\sigma} = G^o_{ij\sigma} + \sum_{l\neq j} G^o_{il\sigma}\Sigma_{l\sigma}\mathcal{G}^o_{lj\sigma} \,. \tag{55}$$

In other words, $\mathcal{G}^o_{ij\sigma}$ embodies the correlation effects due to the medium around the site under consideration.

Our first goal is to show that the local Green's function $G_{ii\sigma}$ satisfies a *local* Dyson equation where the non-interacting propagator $G^o$ is formally replaced by the auxiliary Green's function $\mathcal{G}^o_{ii\sigma}$:

$$G_{ii\sigma} = \mathcal{G}^o_{ii\sigma} + \mathcal{G}^o_{ii\sigma}\,\Sigma_{i\sigma}\,G_{ii\sigma} \,. \tag{56}$$

We start by iterating Eq. (55) to get a series of the form

$$\begin{aligned}
\mathcal{G}^o_{ij\sigma} &= G^o_{ij\sigma} + \sum_{l_1\neq j} G^o_{il_1\sigma}\Sigma_{l_1\sigma}G^o_{l_1j\sigma} + \cdots \\
&= G^o_{ij\sigma} + \sum_{n=1}^{\infty}\sum_{l_1\neq j}\sum_{l_2\neq j}\cdots\sum_{l_n\neq j} G^o_{il_1\sigma}\Sigma_{l_1\sigma}\cdots\Sigma_{l_n\sigma}G^o_{l_nj\sigma} \,.
\end{aligned} \tag{57}$$

Clearly, iterating the full Dyson equation for $G_{ij\sigma}$ generates a similar formal expansion with the only difference that the restriction in the lattice sums in Eq. (57) is completely removed.

Consider now carrying out the same formal expansion for the local Dyson equation we are trying to establish, Eq. (56),

$$\begin{aligned}
G_{ii\sigma} &= \mathcal{G}^o_{ii\sigma} + \mathcal{G}^o_{ii\sigma}\Sigma_{i\sigma}\mathcal{G}^o_{ii\sigma} + \cdots \\
&= \mathcal{G}^o_{ii\sigma} + \sum_{n=1}^{\infty}\mathcal{G}^o_{ii\sigma}\Sigma_{i\sigma}\cdots\Sigma_{i\sigma}\mathcal{G}^o_{ii\sigma} \,,
\end{aligned} \tag{58}$$

and substituting the series in Eq. (57) (with $i = j$) for each occurrence of $\mathcal{G}^o_{ii\sigma}$ in Eq. (58). Let us now regroup all the terms in Eq. (58) with the same number of $\Sigma$. The zero-th order term is clearly $G^o_{ii\sigma}$. To see how things work for higher order terms, consider all the contributions with *one* $\Sigma$ only. Clearly, these can only be originated from the first and second terms in the right hand side of Eq. (58), and read

$$\begin{aligned}
[\text{Terms with one } \Sigma] &= \sum_{l_1\neq i} G^o_{il_1\sigma}\Sigma_{l_1\sigma}G^o_{l_1i\sigma} + G^o_{ii\sigma}\Sigma_{i\sigma}G^o_{ii\sigma} \\
&= \sum_{l_1} G^o_{il_1\sigma}\Sigma_{l_1\sigma}G^o_{l_1i\sigma} \,,
\end{aligned} \tag{59}$$

i.e. the unrestricted lattice sum appearing in the formal expansion of $G_{ii\sigma}$ is recovered. Similarly, by focusing on all the terms with $n$ appearances of $\Sigma$, we realize that all the restrictions in the lattice sums are removed and we get the formal expansion for the local Green's function, which concludes the argument.

Reducing the calculation of $G_{ii\sigma}$ to the local problem in Eq. (56) is the big simplification achieved in infinite dimensions due to the locality of the self-energy. One can in principle use all the tools developed to treat a single-impurity Anderson problem, except that we still lack of a prescription for calculating the auxiliary local Green's function $\mathcal{G}^o_{ii\sigma}$. To close the loop, we consider once again the full Dyson equation for $G$, this time in k-space. It reads:

$$\hat{G}_{\mathbf{k}\sigma} = ([\hat{G}^o_{\mathbf{k}\sigma}]^{-1} - \hat{\Sigma}_\sigma)^{-1} \tag{60}$$

where we have used a $2\times2$ matrix notation to treat the various components $(AA, AB, ...)$ in a compact way. The local Green's function, on the other hand, is simply given by the sum over the Brillouin zone of the appropriate component of $\hat{G}_{\mathbf{k}\sigma}$, i.e.

$$\begin{aligned} G_{ii\sigma} &= \frac{1}{N}\sum_{\mathbf{k}}^{BZ}[\hat{G}_{\mathbf{k}\sigma}]_{\alpha\alpha} \\ &= \frac{1}{N}\sum_{\mathbf{k}}^{BZ}\left[[(\hat{G}^o_{\mathbf{k}\sigma})^{-1} - \hat{\Sigma}_\sigma]^{-1}\right]_{\alpha\alpha} , \end{aligned} \tag{61}$$

where the symbol $\alpha$ stands for the sublattice ($\alpha = A$ or $B$) to which site $i$ belongs. An explicit calculation shows that the dependence on $\mathbf{k}$ of the right hand side of Eq. (61) is contained exclusively in the band energy $E_{\mathbf{k}}$, allowing us to rewrite the sum over $\mathbf{k}$ into an integral involving the non-interacting density of states $\rho(E)$. Explicitly, after some simple algebra one arrives at

$$G_{ii\sigma}(i\omega_n) = \int_0^\infty dE\ \rho(E)\ \frac{Z^{\bar{\alpha}}_\sigma}{Z^A_\sigma Z^B_\sigma - E^2} , \tag{62}$$

where

$$Z^\alpha_\sigma = i\omega_n + \mu + (-1)^R\sigma H_S - \Sigma^{(\alpha)}_\sigma(i\omega_n) , \tag{63}$$

and $\bar{\alpha}$ denotes sublattice $B$ is $\alpha = A$ and viceversa. Notice that in the above equations we have allowed for the presence of a staggered magnetic field $H_S$ which is useful to calculate the staggered susceptibilty of the system using only single-particle quantities.

Eqs. (56,62) are the required relations which allow us to solve the problem *iteratively* given a method for calculating $\Sigma_\sigma$ from a fictitious non-interacting $\mathcal{G}^o$, as explained in the text.

# References


[1] W. Metzner and D. Vollhardt, Phys. Rev. Lett. **62**, 324 (1989)

[2] M. Jarrel, Phys. Rev. Lett. bf 69, 168 (1992)

[3] M. J. Rozenberg, X. Y. Zhang, and G. Kotliar, Phys. Rev. Lett. **69**, 1236 (1992).

[4] A. Georges and W. Krauth, Phys. Rev. Lett. **69**, 1240 (1992).

[5] S. Sorella and E. Tosatti, Europhys. Lett. **19**, 699 (1992).

[6] A. Georges and G. Kotliar, Phys. Rev. B **45**, 6479 (1992)

[7] E. Müller-Hartmann, Z. Phys. B **74**, 507 (1989)

[8] J. E. Hirsch and R. M. Fye, Phys. Rev. Lett. **56**, 2521 (1986)

[9] A. Georges and W. Krauth, preprint (1992).

[10] E. Müller-Hartmann, Z. Phys. B **76**, 211 (1989)

[11] A model on fully connected lattice with randomness in the hopping parameters which completely inhibits AF long range order has been discussed by A. Georges in Ref. [9].

# ACKNOWLEDGEMENTS

My particular thanks go to G. Santoro for all the work he has done and for discussing patiently. I would like to thank S. Sorella for his valuable contribution and for interesting discussions. I am also extremely grateful to E. Tosatti whose helpful remarks and stimulating comments have led to many improvements to this thesis.

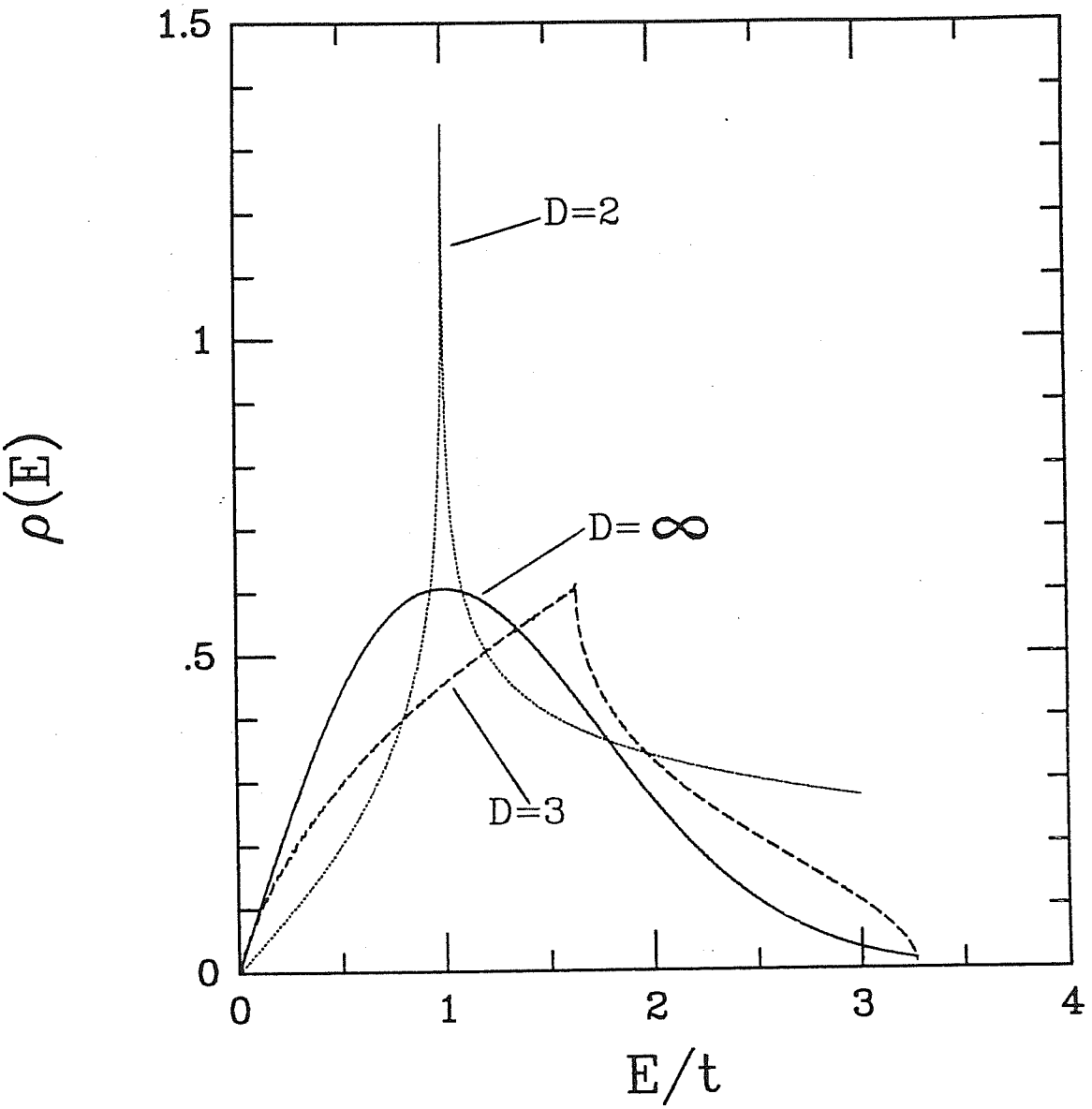


Figure 1

Comparison between the non-interacting density of states for the honeycomb ($D = 2$) and diamond ($D = 3$) lattices and the $D = \infty$ result.

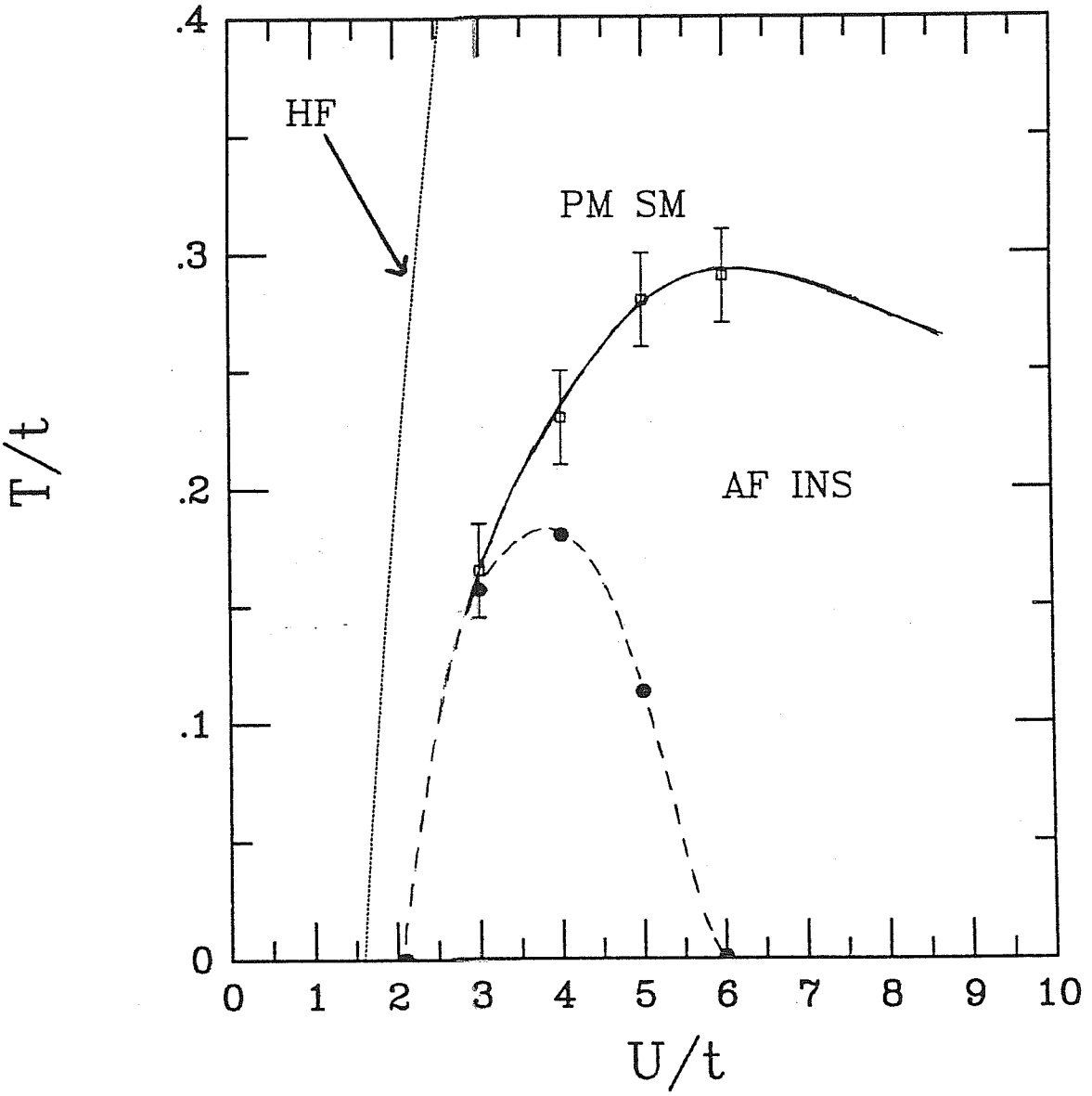


Figure 2

Preliminary phase diagram for the Hubbard model on the $D = \infty$ hyper-diamond lattice at half filling. The dotted line shows the mean-field (Stoner) results for the Neel temperature versus $U$. The solid circles and open squares represent the results for $T_N$ obtained, respectively, with the perturbative and the QMC approaches. The dashed and solid lines are just guides for the eye. "PM SM" and "AF INS" stand, respectively, for "Paramagnetic Semimetal" and "Antiferromagnetic Insulator".

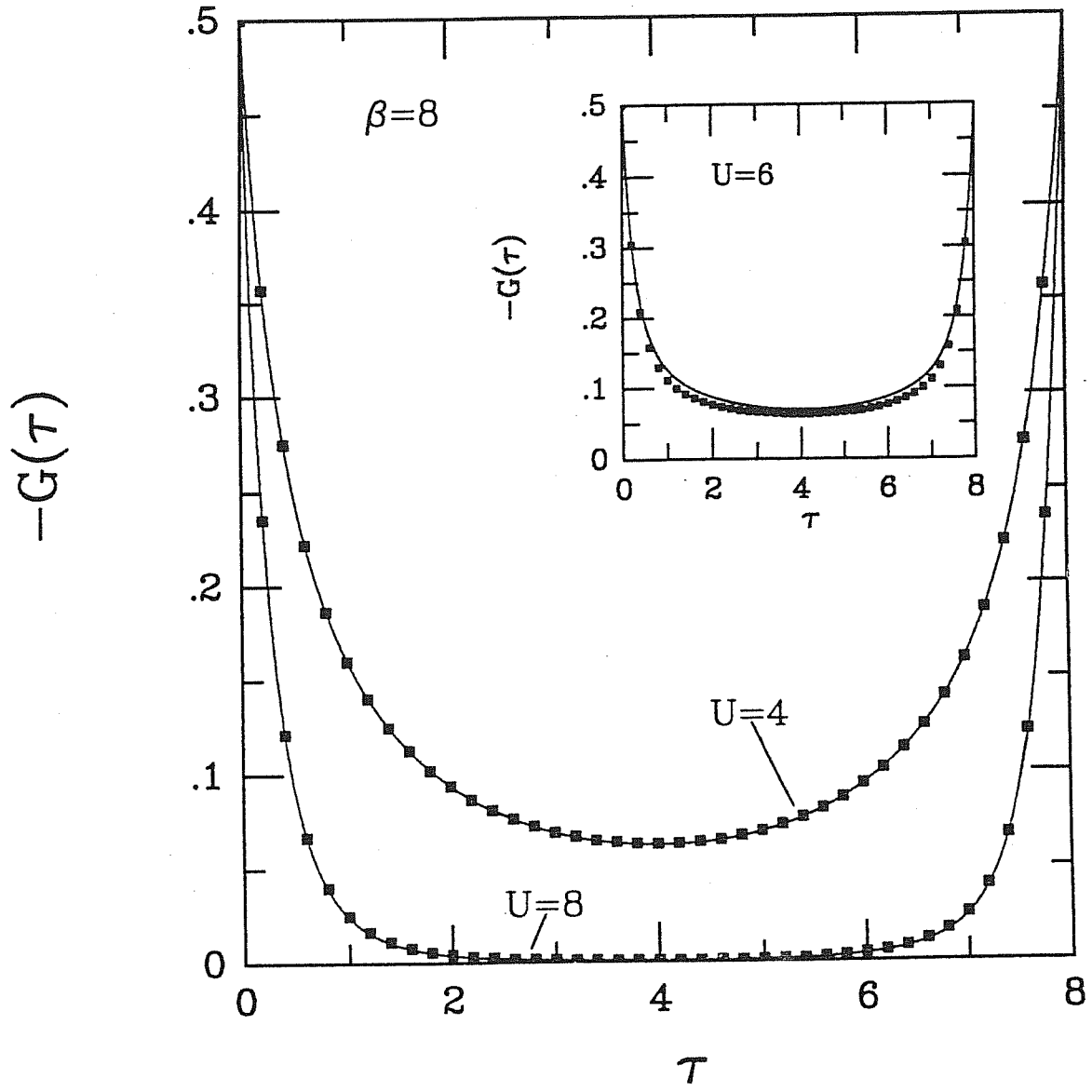


Figure 3

Comparison between the QMC (solid squares) and the perturbative (solid lines) results for the paramagnetic imaginary time local Green's function for several values of $U$ and $\beta = 8$.

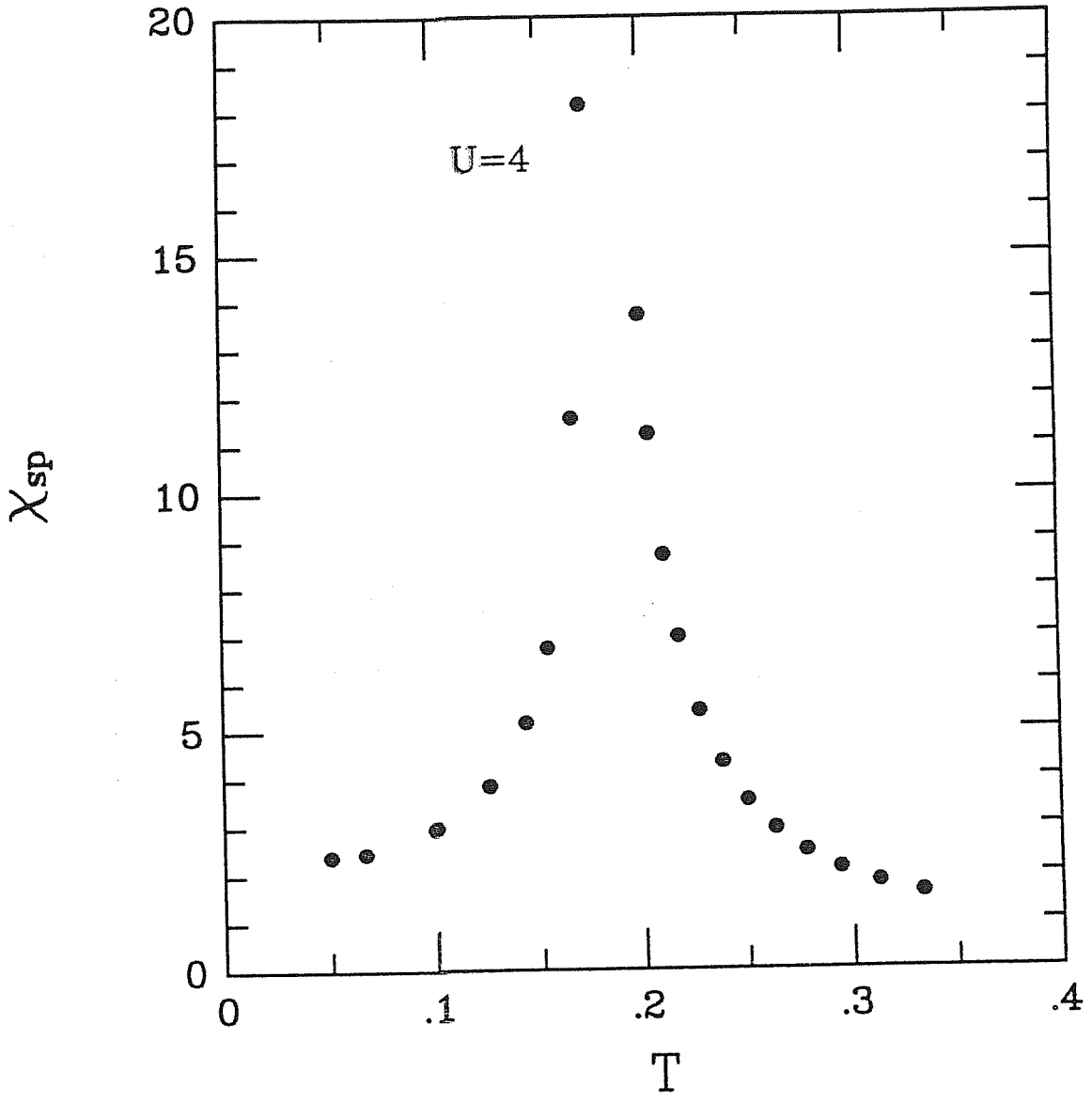


Figure 4

The staggered susceptibility as a function of $T$ for $U/t = 4$. The calculation is performed using the perturbative approach. The critical exponent coincides with the mean-field Ginzburg-Landau value $\gamma = 1$.

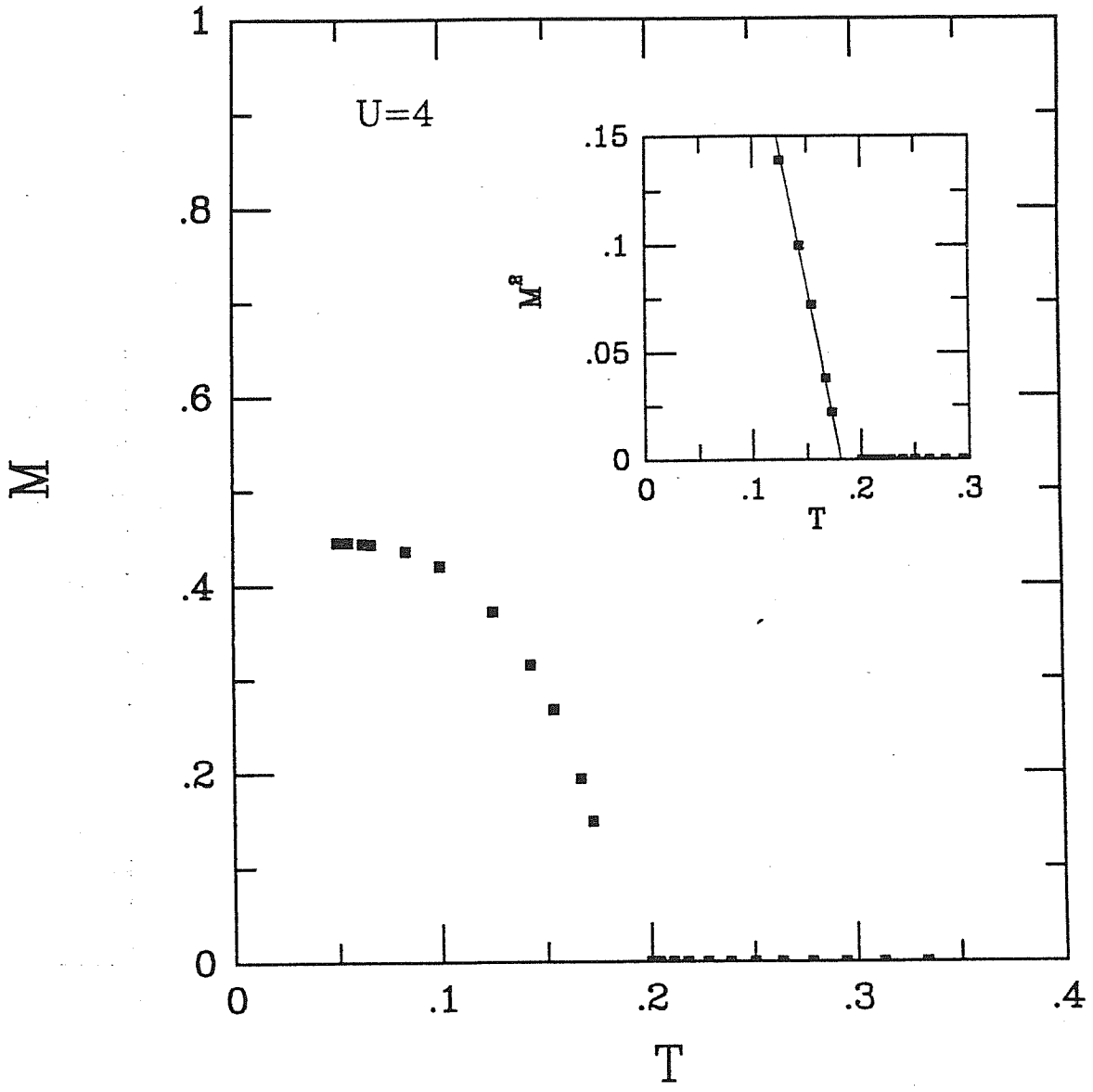


Figure 5

The spontaneous staggered magnetization as a function of $T$ for $U/t = 4$. The critical exponent coincides with the mean-field Ginzburg-Landau value $\beta = 1/2$.

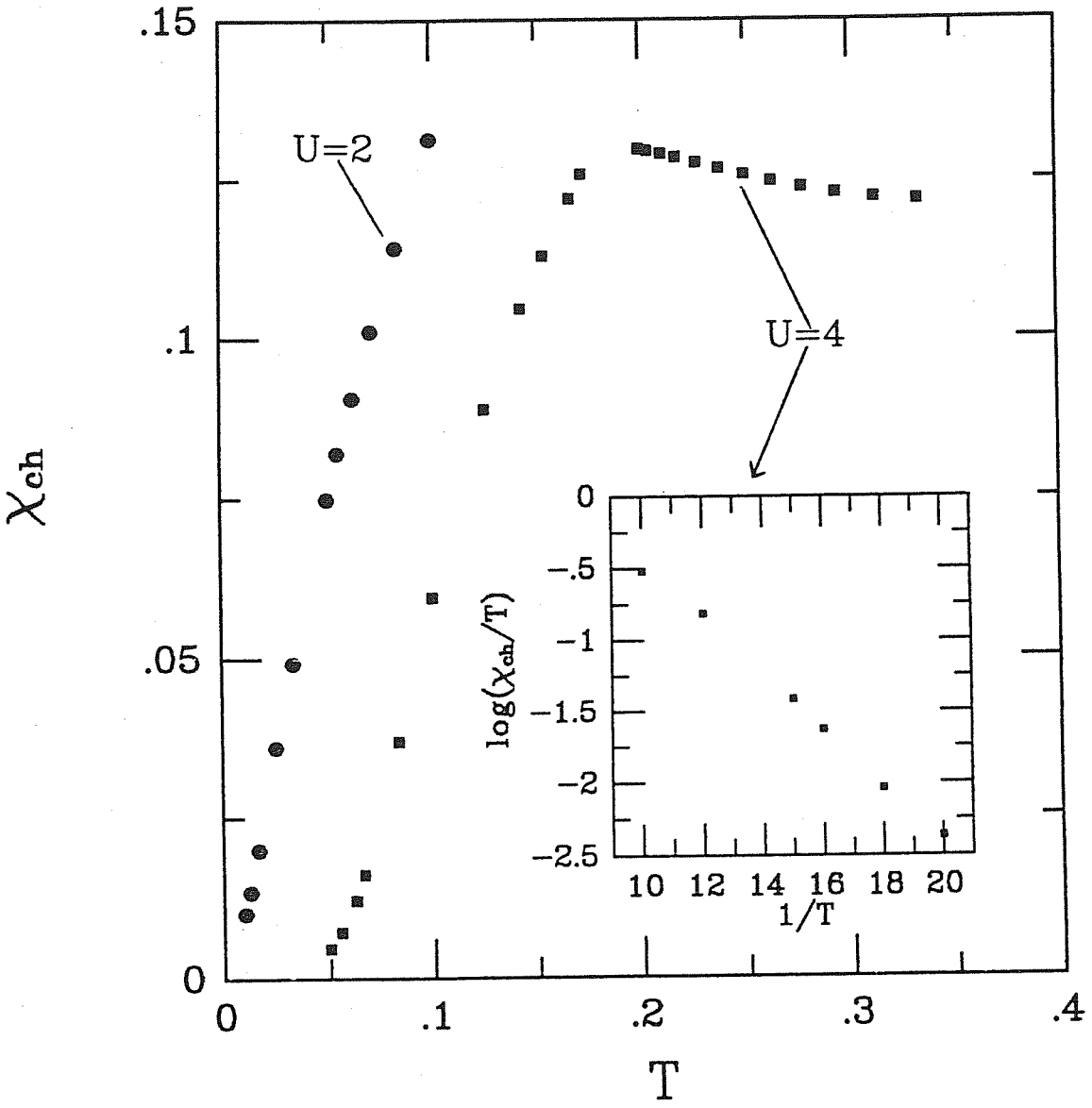


Figure 6

Compressibility $\partial n/\partial \mu$ at half-filling versus $T$ for two values of $U$. For $U/t = 4$ the compressibility shows the presence of a gap in the spectrum, whereas for $U/t = 2$ the typical semimetallic linear behaviour in $T$ is obtained.